



Title	Fluorescence photoswitching of a diarylethene-perylenebisimide dyad based on intramolecular electron transfer
Author(s)	Fukaminato, Tuyoshi; Tanaka, Masaaki; Doi, Takao; Tamaoki, Nobuyuki; Katayama, Tetsuro; Mallick, Arabinda; Ishibashi, Yukihide; Miyasaka, Hiroshi; Irie, Masahiro
Citation	Photochemical & Photobiological Sciences, 9(2), 181-187 https://doi.org/10.1039/b9pp00131j
Issue Date	2010-02
Doc URL	http://hdl.handle.net/2115/44780
Rights	Photochem. Photobiol. Sci., 2010, 9, 181-187 - Reproduced by permission of The Royal Society of Chemistry (RSC)
Type	article (author version)
File Information	PPS9-2_181-187.pdf



[Instructions for use](#)

Fluorescence Photoswitching of a Diarylethene-Perylenebisimide Dyad based on Intramolecular Electron Transfer

Tuyoshi Fukaminato,^{*,†,‡} Masaaki Tanaka,[⊥] Takao Doi,[⊥] Nobuyuki Tamaoki,[†]
Tetsuro Katayama,[‡] Arabinda Mallick,[‡] Yukihide Ishibashi,[‡] Hiroshi Miyasaka^{*,‡}
and Masahiro Irie^{*,§}

[†]*Research Institute for Electronic Science, Hokkaido University, N20, W10, Kita-ku, Sapporo 001-0020, Japan*

[‡]*PREST, Japan Science and Technology Agency (JST)*

[⊥]*Department of Chemistry and Biochemistry, Graduate School of Engineering, Kyushu University, Motoooka 744, Nishi-ku, Fukuoka 819-0395, Japan*

[‡]*Division of Frontier Materials Science, Graduate School of Engineering Science, and Center for Quantum Science and Technology under Extreme Conditions, Osaka University, Toyonaka, Osaka 560-8531, Japan*

[§]*Department of Chemistry and Research Center for Smart Molecules, Rikkyo University, Nishi-Ikebukuro 3-34-1, Toshima-ku, Tokyo 171-8501, Japan*

Received:

**Corresponding authors:*

E-mail: tuyoshi@es.hokudai.ac.jp; miyasaka@chem.es.osaka-u.ac.jp; iriem@rikkyo.ac.jp

Phone & Fax: +81-11-706-9350; +81-6-6850-6241; +81-3-3985-2397

Abstract

A fluorescent photochromic molecule, which is composed of a photochromic diarylethene (DE) and a fluorescent perylenebisimide (PBI), was synthesized and its fluorescence photoswitching was studied. The fluorescence quantum yield of the open-ring isomer is constant irrespective of solvent polarity, while that of the closed-ring isomer decreases with an increase in the dielectric constant of solvents. Femtosecond time-resolved transient and fluorescence lifetime measurements revealed that the fluorescence quenching of the closed-ring isomer is attributed to the intramolecular electron transfer from the PBI chromophore to the DE unit.

Introduction

Fluorescent photochromic molecules have attracted increasing interests owing to their potential applications to optical data storages, molecular switches, fluorescent biological markers, and super high-resolution fluorescence images.¹⁻⁴ Among them, diarylethene based fluorescent photochromic molecules are the most promising candidates for the applications because of their thermal stability and fatigue resistant properties.⁵ Fluorescent diarylethene molecules, in which a fluorescent chromophore is linked to a diarylethene (DE) unit, frequently utilize an intramolecular energy transfer as the fluorescence quenching mechanism.⁶ The excited energy of the fluorescent chromophore is intramolecularly transferred to the photogenerated closed-ring isomer and the fluorescent state is quenched. The process inherently excites the closed-ring isomer of the DE unit and induces the photochromic reaction. To avoid such inconvenient reaction, it is required to employ a new fluorescent quenching mechanism. One of the possible mechanisms is an intramolecular electron-transfer (IET).^{7,8} When the fluorescence can be quenched by the change of oxidation/reduction potentials of the DE unit along with the photochromic reaction and the absorption bands of both DE isomers are shorter than the fluorescence spectrum of the fluorescent chromophore, the quenching does not influence the photochromic reaction. According to the above concept, several fluorescent diarylethene derivatives have been synthesized.⁹ Although the derivatives showed the intramolecular electron-transfer quenching, their quenching efficiency, quantum yield of fluorescence and photochromic reactivity are low. After several trials, we found a diarylethene-perylenebisimide dyad (**1**) (Scheme

1) exhibits reversible and efficient fluorescence switching.¹⁰ Here we report on the fluorescence photoswitching behavior and the detail mechanism of fluorescence quenching process of dyad **1**.

Results and Discussion

Synthesis and Fluorescence Photoswitching

A perylenebisimide (PBI) derivative was chosen as the fluorescent unit because of its photochemical stability, high fluorescence quantum yield, and large molar extinction coefficient.¹¹ A diarylethene (DE) derivative with dioxidized thiophen rings was chosen as the photoswitching unit (Scheme 1).¹² The closed-ring isomer of the diarylethene derivative has an absorption edge slightly shorter than that of the open-ring isomer, as shown in Figure 1.

The synthetic route of the dyad **1** and model diarylethene molecule **2** is illustrated in Scheme 2. Non-symmetric amino-substituted diarylethene derivative **11** was prepared from 2-fluoro-1-(2'-methyl-benzo[*b*]thiophene-3-yl)perfluorocyclopentene (**5**). Compound **7** was obtained by nitration of **5** and continuous reduction. For coupling with **9**, primary amino group of **7** was protected by treating with acetylacetone to form pyrrole substituent, and after coupling of **8** and **9**, the pyrrole was cleaved to reform primary amino group **11**. **11** and *N*-(1-hexylheptyl)perylene-3,4:9,10-tetracarboxyl-3,4-anhydride-9,10-imide (**4**) were linked by condensation in quinoline, with zinc acetate as a Lewis acid catalyst. Finally, compounds **12** and **13** were oxidized with *m*-chloroperoxybenzoic acid (MCPBA) to give

1 and **2**, respectively. Purification was carried out by silica-gel-column chromatography, gel-permeation chromatography (GPC), and high-performance liquid chromatography (HPLC). The structures of all molecules were identified by ^1H NMR, mass spectrum, and elemental analysis. Detailed synthetic procedures and compound data are described in Electronic Supplementary Information (ESI).

Figure 1 shows the absorption spectral changes along with the photocyclization and photocycloreversion reactions of **2** in 1,4-dioxane. Before photoirradiation, the absorption maximum and the absorption edge are observed at 355 nm and 470 nm, respectively. Upon irradiation with visible light ($\lambda = 445$ nm), a new absorption band having the maximum at 365 nm and the edge at 450 nm grows up in UV region, though the increase of the absorption is minute. Upon irradiation with UV (365 nm) light, the absorption band returned to the initial one. The absorption spectrum of the closed-ring isomer (**2b**) is also shown in Figure 1. The photoconversion from **2a** to **2b** at the photostationary state under irradiation with 445 nm light was estimated to be 6 % from the absorption spectra.

Figure 2a and 2b show the absorption and fluorescence spectral changes upon irradiation with visible ($\lambda = 445$ nm) and UV (365 nm) light in 1,4-dioxane ($\epsilon = 2.21$) of **1**, respectively. Upon $\lambda = 445$ nm light irradiation, the absorption band in 300-400 nm region gradually increases, while any fluorescence intensity change was not observed. This result suggests that an intramolecular singlet-singlet energy transfer from the PBI unit to the DE unit does not occur. In actual, the fluorescence spectrum of the PBI unit has no overlaps with the absorption spectra of both isomers of the DE unit and supports

no effective singlet-singlet intramolecular energy transfer from the PBI unit to the DE unit. Upon irradiation with UV (365 nm) light, the absorption band turned back to the initial one. From the absorption spectrum of **1b** isolated by HPLC, the conversion from **1a** to **1b** in the photostationary state upon irradiation with 445 nm light was estimate to be 91 %.

On the other hand, in a binary mixture solvent of 1,4-dioxane and methanol (50/50) ($\epsilon = 17.4$), the fluorescence intensity decreases along with the photocyclization reaction (Figure 2c and 2d). At the photostationary state under irradiation with 445 nm light, the fluorescence quantum yield decreases from 0.91 to 0.19. The fluorescence intensity recovered upon UV (365 nm) light irradiation. The fluorescence switching can be repeated more than 10 times. This solvent effect suggests that the fluorescence quenching is caused by IET.

In order to confirm the IET process of **1**, the absolute fluorescence quantum yields of both **1a** and **1b** were measured as a function of solvent dielectric constant. In high dielectric constant solvents the IET process becomes dominant because of the stabilization of the charge separated states. Figure 3 and Table 1 show the dependence of the fluorescence quantum yields of two isomers on the dielectric constant (ϵ) of solvents at room temperature. As can be seen from Figure 3, **1a** has a constant fluorescence quantum yield ($\Phi_F \sim 0.9$) irrespective of solvent polarity. In contrast, Φ_F of **1b** is strongly dependent on the dielectric constant of solvents. The closed-ring isomer (**1b**) is strongly fluorescent ($\Phi_F \sim 0.8$) in pure 1,4-dioxane, while Φ_F decreases, down to $\Phi_F = 0.12$ in the binary solvent of 1,4-dioxane and methanol (30/70) ($\epsilon = 23.5$). The

shape and position of the absorption and fluorescence spectra are almost similar in all solvents. The solvent dependence of Φ_F indicates that IET takes place only for the closed-ring isomer.¹³

The energy gap (ΔG°) for the charge separation reaction in the excited state of both isomer of **1** in a given solvent can be estimated from oxidation and reduction potentials of model diarylethene **2** and perylenebisimide **3** by using Rehm-Weller Equation (eq. 1).

$$\Delta G^\circ (eV) = e(E_{ox} - E_{red}) - (E_{00}) - \frac{e^2}{4\pi\epsilon_0\epsilon_s R_{cc}} - \frac{1}{8\pi\epsilon_0} \left(\frac{1}{r^+} + \frac{1}{r^-} \right) \left(\frac{1}{\epsilon_{ref}} - \frac{1}{\epsilon_s} \right) \quad (1)$$

$E_{ox}(D)$ and $E_{red}(A)$ are the first oxidation potential of the donor PBI and first reduction potential of the acceptor DE, respectively. E_{00} is the spectroscopic excited state energy, while R_{cc} is the distance between the centers of the donor and acceptor moieties. The effective ionic radii of the donor radical cation and the acceptor radical anion are labeled as r^+ and r^- , respectively. The dielectric constant of the reference solvent used in electrochemistry is denoted as ϵ_{ref} , while ϵ_s is the dielectric constant of the given solvent.

From the absorption and fluorescence spectra of **1** recorded in dichloromethane, S_0 - S_1 excitation energy is estimated to be 2.34 eV. The redox potentials of **2a**, **2b** and **3** were obtained by cyclic voltammograms (CV) in dichloromethane to be -1.39 V, -0.97 V and 1.23 V, respectively, with ferrocene as an internal reference (see ESI). Donor-acceptor distances of 12.1 Å and 12.8 Å are estimated from the optimized geometries of **1a** and **1b** conjugates, respectively.¹⁴ By applying these values to eq. 1, ΔG° value for open-ring and closed-ring isomer are estimated to be +0.28 eV and -0.15 eV, respectively. From these values, the electron transfer process is thermodynamically

feasible only for the closed-ring isomer (**1b**). In more polar solvents, the charge separated state of **1b** becomes more stable and IET process becomes more favorable.

Transient Spectroscopic Measurements

To directly study the fluorescence quenching mechanism, time-resolved fluorescent and transient absorption spectroscopies were carried out.

Figure 4a and 4b show the fluorescence time profiles of **1a** in pure 1,4-dioxane and in the binary solvent (1,4-dioxane/methanol = 50/50) as a reference. The time profiles of **1a** in both solutions show a single-exponential decay with a time constant of (3.7 ± 0.1) ns. This decay time constant is in good agreement with the fluorescence lifetime of PBI in ethanol.¹⁵ Figure 4c and 4d show fluorescence time profiles of **1b** in pure 1,4-dioxane and in the binary solvent (1,4-dioxane/methanol = 50/50). The time profile of **1b** in 1,4-dioxane shows a single-exponential decay with the time constant of (3.7 ± 0.1) ns. The identical lifetime indicates that the fluorescence of PBI is not affected by the closed-isomer of the DE unit in **1b** in pure 1,4-dioxane. On the other hand, the time profile of **1b** in the binary solvent shows rapid decay in sub-ns time region. The red solid line in the figure is the curve calculated with a double-exponential function with the faster time constant of (700 ± 50) ps and the slower one of (3.7 ± 0.1) ns. Preexponential factors for the faster and the slower time constants were obtained to be 0.95 and 0.05, respectively. The fast decay of (700 ± 50) ps indicates that the PBI in the fluorescent state is effectively quenched by the closed-form of the DE unit in **1b** in the binary solvent. On the other hand, the smaller

component with the lifetime of (3.7 ± 0.1) ns may be attributed to the decay of the small amount of PBI moiety with the open form remaining in the solution. The same time constants and preexponential factors were obtained for the time profiles of both **1a** and **1b** in pure 1,4-dioxane and the binary solvent monitored at 575 nm.

The transient absorption spectra of **1b** were measured by using a femtosecond laser pulse. Figure 5a shows the result of **1b** in pure 1,4-dioxane solution. Immediately after the excitation, a negative signal in the wavelength region of 450-600 nm appears together with a positive signal in the wavelength regions > 620 nm. The negative signal in the region of 450-550 nm is assigned to the depletion of the ground state of PBI moiety in **1b**. On the other hand, the negative signal around 550-600 nm and the positive band with a maximum at ca. 680 nm can be assigned to the stimulated emission and the S_1 state of the PBI moiety, respectively.¹⁶ The absorption spectrum gradually decreases while keeping the spectral band shape unchanged. On the other hand, the time-resolved spectra of **1b** in the binary solvents (1,4-dioxane/methanol = 50/50) are shown in Figure 5b. As can be seen from Figure 5a, the rapid appearance of the S_1 state of the PBI moiety is followed by the decay in sub-ns to ns time region. The decay of the spectrum in the entire wavelength region is, however, much faster than that observed in Figure 5a.

In order to analyze the temporal evolution of the transient absorption signals of **1b**, we plotted time profiles at various wavelengths in Figure 6. Results in pure 1,4-dioxane solution are shown in Figure 6a – d, while those in the polar binary solvent are shown in Figure 6e – h. The monitoring wavelengths are 470 nm (the depletion of

the ground state of **1b**), 570 nm (the stimulated emission), 620 nm and 680 nm (the positive signal), respectively. All the time profiles for **1b** in 1,4-dioxane solution, Figure 6a - d, are reproduced by a single-exponential function with a time constant of 3.7 ns, indicating again that the transient absorption spectrum is safely ascribed to the S₁ state of PBI moiety.

On the other hand, time profiles in the polar binary solvent are rather complicated. At 470 nm where the ground state of PBI moiety has an absorption band, the quick appearance of the negative signal is followed by the recovery. This time profile was reproduced by a double-exponential function with the faster time constant of 680 ps and the slower one of 3.7 ns. The preexponential factors for the faster and the slower components are 0.88 and 0.12, respectively. By integrating the time profiles of the fluorescence in Figure 4, the faster time constant can be assigned to the decay of the S₁ state of PBI moiety via the quenching process in **1b**, while the slower one can be attributed to the decay of the small amount of PBI moiety with the open form remaining in the solution because this time constant was in agreement with that of the slower component in the fluorescence decays. Similar double-exponential time profile is confirmed at 680 nm. On the other hand, at 570 and 620 nm, much faster process was observed in addition to these two components. The time profiles at 570 nm and 620 nm are analyzed by a triple-exponential function with the time constants of (80 ± 5) ps, (660 ± 30) ps, and (3.7 ± 0.1) ns. Because the time constants for the second (660 ps) and the third (3.7 ns) components are similar to those observed in the fluorescence decay process and time profiles of the transient absorbance at 470 nm and 680 nm, these

two components can be attributed to the decay of the S₁ state.

To elucidate the fast time constant of 80 ps, we analyzed the transient absorption spectrum on the basis of the sequential reaction processes as $A \rightarrow B \rightarrow C$ shown in Scheme 3. Here, A , B and C indicate the S₁ state of the PBI moiety, the transient species produced by the quenching process, and the ground state of **1b**, respectively. By analyzing the time profiles of the transient absorbance at every monitoring wavelength with the use of eq. 2 (See Electronic Supplementary Information for the derivation of eq. 2), we can obtain the wavelength dependence of the relative values of ε_A^λ and ε_B^λ , corresponding to the absorption spectra the species A and B .

$$\Delta A(t) = [A(0)] \left\{ \left(\varepsilon_A^\lambda + \varepsilon_B^\lambda \frac{k_q}{k_2 - k_1} \right) \exp[-k_1 t] - \left(\varepsilon_B^\lambda \frac{k_q}{k_2 - k_1} \right) \exp[-k_2 t] \right\} \quad (2)$$

Here, the rate constant, k_1 is the summation of k_q and k_f , where the k_q and k_f are respectively the quenching constant and the reciprocal value of the fluorescent lifetime of the PBI moiety. In the actual analysis, $(k_1)^{-1}$ and $(k_2)^{-1}$ of eq. 2 are set to be 660 and 80 ps, as obtained by the transient absorption spectroscopy and the k_q value of $1.24 \times 10^9 \text{ s}^{-1}$ was used as the difference between the time constants of $(3.7 \text{ ns})^{-1}$ and $(660 \text{ ps})^{-1}$. The long component of 3.7 ns was subtracted in the analysis.

Figure 7 shows the relative values of ε_A^λ and ε_B^λ in the wavelength region of 550-750 nm. The spectrum for A (open circles) is identical with the S_n ← S₁ absorption spectrum obtained for **1b** in 1,4-dioxane solution (solid line), ensuring the validity of the present analysis. The spectrum with the absorption maximum around 570 nm can be assigned to species B (closed circles). This band shape and the absorption maximum are close to those of the cation radical of PBI.¹⁷ The result

indicates that species *B* is the charge-separated state between the PBI chromophore and the closed-ring isomer of the DE unit. As shown in Scheme 3, the singlet excited state of **1b** (species *A*) converts to the charge separated state (species *B*) with the time constant of 660 ps in the binary solvent and the charge recombination to the ground state (species *C*) takes place with a 80-ps time constant.

It is worth to note that illumination at 500 – 550 nm region, where only the PBI chromophore has absorption and the DE unit has no absorption, induces the photocyclization reaction of the DE unit via triplet state, as reported in a previous paper.^{9c} Although we failed to demonstrate a perfect non-destructive readout performance because of the presence of the triplet photocyclization route, the photocycloreversion reaction along with the energy transfer quenching is successfully avoided in the present dyad.

Conclusions

A photoswitchable fluorescent molecule, which is composed of a photochromic DE and a fluorescent PBI, was synthesized and its fluorescence photoswitching was studied. Although the fluorescence quantum yield of **1a** is not affected by the solvent polarity, that of **1b** is strongly dependent on the solvent polarity and it decreases with an increase in solvent dielectric constant. The result indicates that the effective quenching of the fluorescence took place only in **1b** in polar solvents. The estimation of the energy level of the charge separated state between DE and PBI units and the direct detection of the

reaction dynamics revealed that the electron transfer from PBI in the excited state to the closed-ring isomer of DE unit is responsible for the fluorescence quenching in **1b**.

Experimental Section

Solvents used in photochemical measurements were of spectroscopic grade and were purified by distillation before use. ^1H NMR spectra were recorded on a NMR spectrometer (Bruker AVANCE 400, 400 MHz). Samples were dissolved in CDCl_3 with tetramethylsilane as an internal standard. Mass spectra were measured with a mass spectrometer (Shimadzu GCMS-QP5050A and JEOL GC mate II). CV was measured by ALS-600 electrochemical analyzer. Absorption and fluorescence spectra were measured with a Hitachi U-3500 absorption spectrophotometer and a Hitachi F-2500 fluorescence spectrophotometer, respectively. Fluorescence quantum yields were determined by using a monochromic 502 nm light as the excitation light source, a very dilute solution, the absorbance of which is less than 0.02 at the excitation wavelength for all solvents, and *N,N'*-bis(1-hexylheptyl)-perylene-3,4:9,10-tetracarboxylbisimide ($\Phi_f = 0.99$) as the reference. Photoirradiation was carried out using an USHIO 1000 W high-pressure mercury lamp or an USHIO 500 W xenon lamp as the light sources. Monochromic light was obtained by passing the light through a monochromator (Jobin-Yvon).

For the detection of dynamic behaviors in femtosecond – nanosecond time region, a dual NOPA/OPA laser system was used for transient absorption measurements. The details of the system were described elsewhere.¹⁸ Briefly, the output of a femtosecond

Ti: Sapphire laser (Tsunami, Spectra-Physics) pumped by the SHG of a cw Nd³⁺:YVO₄ laser (Millennia V, Spectra-Physics) was regeneratively amplified with 1 kHz repetition rate (Spitfire, Spectra-Physics). The amplified pulse (802 nm, 0.9 mJ/pulse energy, 85 fs fwhm, 1 kHz) was divided into two pulses with the same energy (50 %). The one of these pulses was guided into NOPA (non-collinear optical parametric amplifier) system (TOPAS-white, Light-Conversion). The NOPA output can cover the wavelength region between 500 and 1000 nm with 1-40 mW output energy with ca. 20 fs fwhm. In the present work, excitation wavelength was set to 530 nm. White light continuum, which was generated by focusing the fundamental light at 802 nm into 1 mm quartz window, covers the wavelength region from 450 to 780 nm. Polarization of two pulses was set at magic angle for all the measurement. The signal and the reference pulses were respectively detected with multichannel photodiode array systems (PMA-10, Hamamatsu) and the detected signals were sent to a personal computer for further analysis. Spectra were calibrated for the group velocity dispersion. From the cross correlation trace between the NOPA output and the super-continuum at the sample position, the response pulse duration was ca. 80 fs. Rotating sample cell with an optical length of 2 mm was utilized and the absorbance of the sample at the excitation wavelength was ~1.0.

For the measurement of the fluorescence time profiles, time-correlated single-photon counting (TCSPC) method using a picosecond Nd³⁺:YAG laser (DPM-1000&SBR-5080-FAP, Coherent, 532 nm, fwhm ca.30 ps) with 8 MHz repetition rate was employed.¹⁹ A photomultiplier tube (Hamamatsu Photonics, R3809U-50)

with an amplifier (Hamamatsu Photonics C5594) and a counting board (PicoQuanta, PicoHarp 300) were used for the signal detection. A monochromator was placed in front of the photomultiplier tube, and the spectral resolution was ca. 2 nm. The system response time was determined to be ca. 32 ps FWHM from a scattered light from a colloidal solution. Sample cell with an optical length of 1 cm was utilized and the absorbance of the sample at 532 nm was ~0.3.

Acknowledgment

This work was partly supported by Grant-in-Aids for Scientific Research on Priority Areas “New Frontiers in Photochromism (471)” (No. 19050008) from the Ministry of Education, Culture, Sports, Science, and Technology (MEXT) of Japanese Government. T. F. acknowledges support from PREST, JST and Grant-in-Aids for Young Scientist (B) (No. 21750149).

References and Notes

- 1) (a) M. Irie, H. Ishida, T. Tsujioka, *Jpn. J. Appl. Phys.*, 1999, **38**, 6114; (b) T. Fukaminato, T. Kawai, S. Kobatake, M. Irie, *Proc. Jpn. Acad.*, 2001, **77**, 30; (c) M. Irie, T. Fukaminato, T. Sasaki, N. Tamai, T. Kawai, *Nature*, 2002, **420**, 759; (d) S.-J. Lim, J. Seo, S. Y. Park, *J. Am. Chem. Soc.*, 2006, **128**, 14542; (e) C. C. Corredor, Z.-L. Huang, K. D. Belfield, A. R. Morales, M. V. Bondar, *Chem. Mater.*, 2007, **19**, 5165.
- 2) (a) *Molecular Switches*; B. L. Feringa, Ed.; Wiley-VCH: Weinheim, 2001; (b) G. H. Brown *Photochromism*; Wiley-Interscience: New York, 1971; (c) H. Durr, H. Bouas-Laurent, *Photochromism: Molecules and Systems*; Elsevier: Amsterdam, 2003.
- 3) (a) E. A. Jares-Erijman, T. M. Jovin, *Nat. Biotech.*, 2003, **21**, 1387; (b) N. Soh, K. Yoshida, H. Nakajima, K. Nakano, T. Imato, T. Fukaminato, M. Irie, *Chem. Commun.*, 2007, 5206; (c) L. Zhu, W. Wu, M.-Q. Zhu, J. J. Han, J. K. Hurst, A. D. Q. Li, *J. Am. Chem. Soc.*, 2007, **129**, 3524; (d) Y. Zou, T. Yi, S. Xiao, F. Li, C. Li, X. Gao, J. Wu, M. Yu, C. Huang, *J. Am. Chem. Soc.*, 2008, **130**, 15750.
- 4) (a) P. Dedecker, J. Hotta, C. Flors, M. Sliwa, H. Uji-i, M. B. J. Roeffaers, R. Ando, H. Mizuno, A. Miyawaki, J. Hofkens, *J. Am. Chem. Soc.*, 2007, **129**, 6132; (b) S. W. Hell, *Science*, 2007, **316**, 1153; (c) M. Heilemann, P. Dedecker, J. Hofkens, M. Sauer, *Laser & Photon. Rev.*, 2009, **3**, 180; (d) D. Hu, Z. Tian, W. Wu, W. Wan, A. D. Q. Li, *J. Am. Chem. Soc.* 2008, **130**, 15279; (e) M. Heilmann, S. van de Linde, M. Schüttpelz, R. Kasper, B. Seefeldt, A. Mukherjee, P. Tinnefeld, M. Sauer, *Angew. Chem. Int. Ed.*, 2008, **47**, 6172.

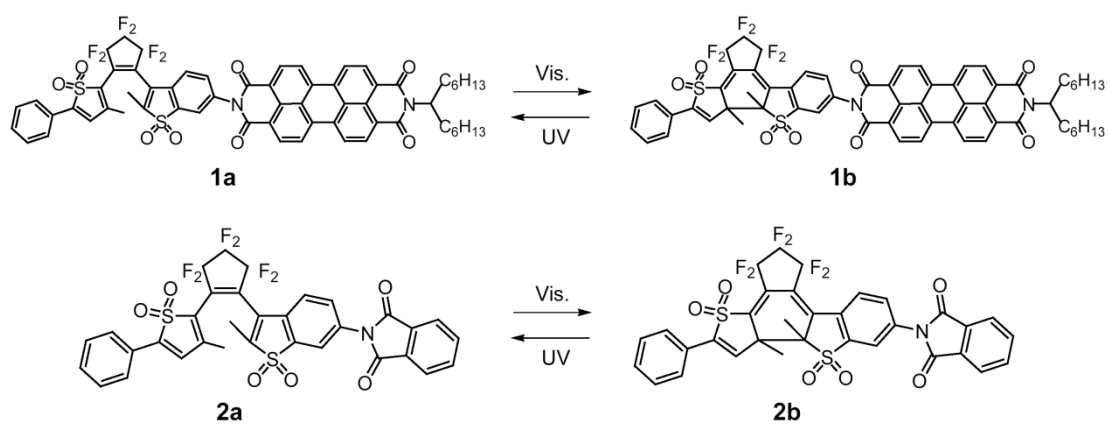
- 5) (a) M. Hanazawa, R. Sumiya, Y. Horikawa, M. Irie, *J. Chem. Soc. Chem. Commun.*, 1992, 206; (b) M. Irie, T. Lifka, K. Uchida, S. Kobatake, Y. Shindo, *Chem. Commun.* 1999, 747; (c) M. Irie, *Chem. Rev.*, 2000, **100**, 1685; (d) S. Nakamura, M. Irie, *J. Org. Chem.*, 1998, **53**, 6136; (e) S. Takami, S. Kobatake, T. Kawai, M. Irie, *Chem. Lett.*, 2003, **32**, 892.
- 6) (a) K. Yagi, C. F. Soong, M. Irie, *J. Org. Chem.*, 2001, **66**, 5419; (b) T. Kawai, T. Sasaki, M. Irie, *Chem. Commun.*, 2001, 711; (c) L. Giordano, T. M. Jovin, M. Irie, E. A. Jares-Erijman, *J. Am. Chem. Soc.* 2002, **124**, 7481; (d) T. Fukaminato, T. Sasaki, N. Tamai, T. Kawai, M. Irie, *J. Am. Chem. Soc.*, 2004, **126**, 14843; (e) M. Bossi, V. Belov, S. Polyakova, S. W. Hell, *Angew. Chem. Int. Ed.*, 2006, **45**, 7462; (f) T. Fukaminato, T. Umemoto, Y. Iwata, S. Yokojima, Y. Yoneyama, S. Nakamura, M. Irie, *J. Am. Chem. Soc.*, 2007, **129**, 5932.
- 7) (a) V. Balzani, F. Scandola, *Supramolecular Photochemistry*, Ellis Horwood : New York, 1991; (b) *Electron Transfer in Chemistry*, V. Balzani, Ed.; Wiley-VCH: Weinheim, 2001.
- 8) (a) S. Tsuchiya, *J. Am. Chem. Soc.* 1999, **121**, 48; (b) J. M. Endtner, F. Effenberger, A. Hartschuh, H. Port, *J. Am. Chem. Soc.*, 2000, **122**, 3037; (c) A. J. Myles, N. R. Branda, *J. Am. Chem. Soc.*, 2001, **123**, 177; (d) P. A. Liddell, G. Kodis, A. L. Moore, T. A. Moore, D. Gust, *J. Am. Chem. Soc.* 2002, **124**, 7668.
- 9) (a) Y. Odo, T. Fukaminato, M. Irie, *Chem. Lett.*, 2007, **36**, 240; (b) M. Berberich, A. M. Krause, M. Orlandi, F. Scandola, F. Wurthner, *Angew. Chem. Int. Ed.*, 2008, **47**, 6616; (c) T. Fukaminato, T. Doi, M. Tanaka, M. Irie, *J. Phys. Chem. C*, 2009, **113**,

- 11623.
- 10) We have reported an unexpected photocyclization reaction of dyad **1** in a recent (see reference 9c).
- 11) H. Langhals, *Helv. Chim. Acta*, 2005, **88**, 1309.
- 12) (a) Y.-C. Jeong, S. I. Yang, K.-H. Ahn, E. Kim, *Chem. Commun.*, 2005, 2503; (b) T. Fukaminato, M. Tanaka, L. Kuroki, M. Irie, *Chem. Commun.*, 2008, 3924.
- 13) Similar solvent dependence has been observed for PBI dimmers; M. W. Holman, R. Liu, L. Zang, P. Yan, S. A. DiBenedetto, R. D. Bowers D. M. Adams, *J. Am. Chem. Soc.*, 2004, **126**, 16126.
- 14) Donor-acceptor distances of both isomers were estimated from the AM1 calculation in MOPAC.
- 15) S. Tinnefeld, G. Calzaferri, *ChemPhysChem*, 2004, **5**, 239.
- 16) (a) H. Lehtivouri, T. Kumpulainen, M. Hietala, A. Efimov, H. Lemmetyinen, A. Kira, H. Imahori, N. V. Tkachenko, *J. Phys. Chem. C*, 2009, **113**, 1984.
- 17) T. Kircher, H. G. Löhmannsröben, *Phys. Chem. Chem. Phys.*, 1999, **1**, 3987.
- 18) (a) H. Miyasaka, M. Murakami, T. Okada, Y. Nagata, A. Itaya, S. Kobatake, M. Irie, *Chem. Phys. Lett.*, 2003, **371**, 40; (b) Y. Ishibashi, M. Murakami, H. Miyasaka, S. Kobatake, M. Irie, Y. Yokoyama, *J. Phys. Chem. C*, 2007, **111**, 2730; (c) Y. Ishibashi, T. Katayama, C. Ota, S. Kobatake, M. Irie, Y. Yokoyama, H. Miyasaka, *New J. Chem.*, 2009, **33**, 1409.
- 19) (a) D. V. O'Connor, D. Philips, "Time-Correlated Single-Photon Counting", Academic Press, London, 1984; (b) Y. Nagasawa, A. Oishi, T. Itoh, M. Yasuda, M.

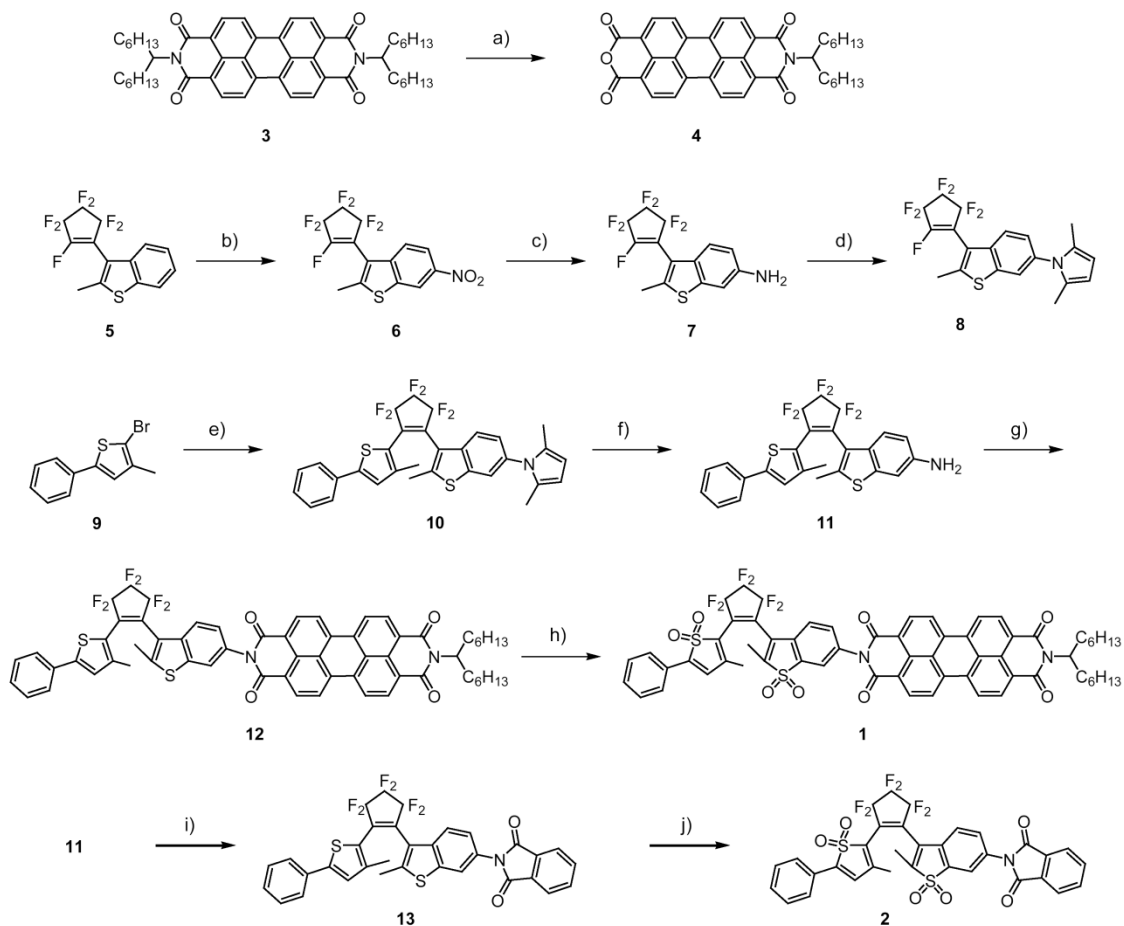
Muramatsu, Y. Ishibashi, S. Ito, H. Miyasaka, *J. Phys. Chem. C.*, 2009, **113**, 11868.

Table 1. Absorption and fluorescence wavelength maxima, and fluorescence quantum yields of the open-ring isomer **1a** and the closed-ring isomer **1b** in mixture solvents having different dielectric constant.

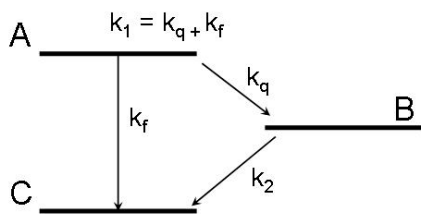
Solvent; 1,4-dioxane/ methanole	Dielectric constant (ϵ)	open-ring isomer (1a)			closed-ring isomer (1b)		
		$\lambda_{\text{max, abs}}$ (nm)	$\lambda_{\text{max, flu}}$ (nm)	Φ_f	$\lambda_{\text{max, abs}}$ (nm)	$\lambda_{\text{max, flu}}$ (nm)	Φ_f
100/0	2.21	524	536	0.91	525	536	0.82
90/10	5.25	523	536	0.89	524	536	0.82
85/15	6.77	523	536	0.89	525	536	0.82
80/20	8.29	524	536	0.90	525	536	0.67
75/25	9.81	523	536	0.90	524	537	0.50
70/30	11.33	524	537	0.90	524	537	0.31
60/40	14.37	524	537	0.89	524	538	0.18
50/50	17.41	524	538	0.91	525	539	0.15
40/60	20.44	524	538	0.88	524	539	0.13
30/70	23.48	524	538	0.88	525	539	0.12



Scheme 1. Photochromism of a DE-PBI dyad **1** and a model DE molecule **2**.



Scheme 2. Synthesis of DE-PBI dyad **1** and model DE molecule **2**: a) KOH, *tert*-BuOH, reflux, 20 min., 58 %; b) fuming HNO₃, AcOH, Ac₂O, 10 °C → r.t., 6h, 55 %; c) NaBH₄, NiCl₂·6H₂O, MeOH, 10 °C → r.t., 1h; d) acetonylacetone, AcOH, toluene, reflux, 14h, 92 %; e) *n*-BuLi, dry THF, -78 °C, 1h → **8**, dry THF, -78 °C, 30 min., 88 %; f) NH₂OH·HCl, NEt₃, EtOH/H₂O, reflux (vigorous), 36h, 89 %; g) **4**, Zn(OAc)₂, quinoline, 155 °C, 20h, 91 %; h) MCPBA, CH₂Cl₂, r.t., 5 days, 34 %; i) phthalic anhydride, Zn(OAc)₂, quinoline, 155 °C, 20h, 92 %; j) MCPBA, CH₂Cl₂, r.t., 37 %.



Scheme 3. Model of a sequential reaction process.

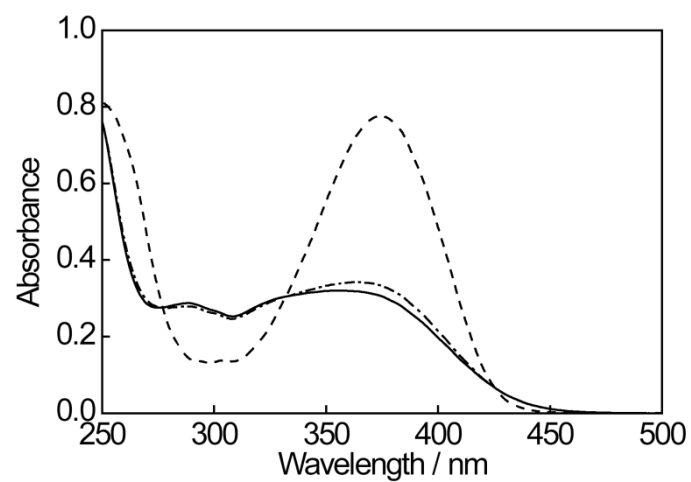


Figure 1. Absorption spectra of **2** in 1,4-dioxane solution; the open-ring isomer (**2a**) (solid line), the closed-ring isomer (**2b**) (dashed line), and the photostationary state under irradiation with 445 nm light (dashed-dotted line).

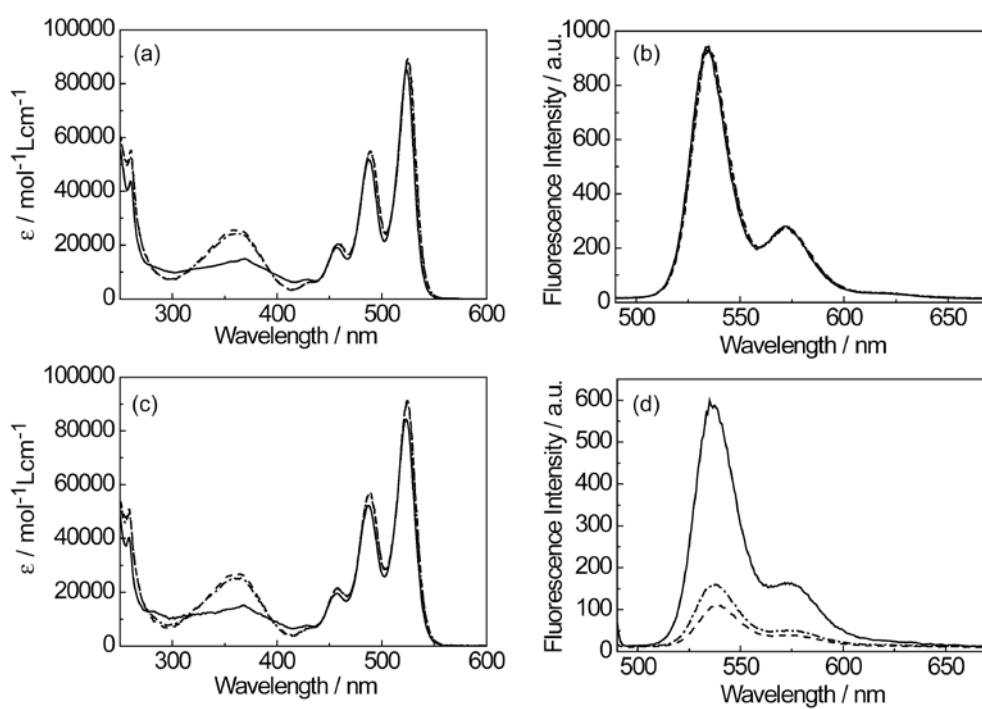


Figure 2. (a) Absorption and (b) fluorescence spectra of **1** in 1,4-dioxane solution, (c) absorption and (d) fluorescence spectra of **1** in a binary solvent (1,4-dioxane/methanol = 50/50); the open-ring isomer (**1a**) (solid line), the closed-ring isomer (**1b**) (dashed line), the photostationary state under irradiation with 445 nm light (dashed-dotted line).

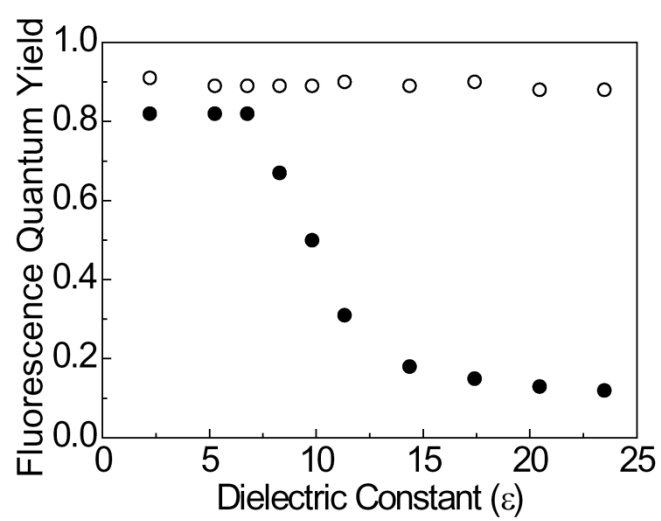


Figure 3. Fluorescence quantum yields as a function of the dielectric constant of solvents for **1a** (open circle) and **1b** (closed circle).

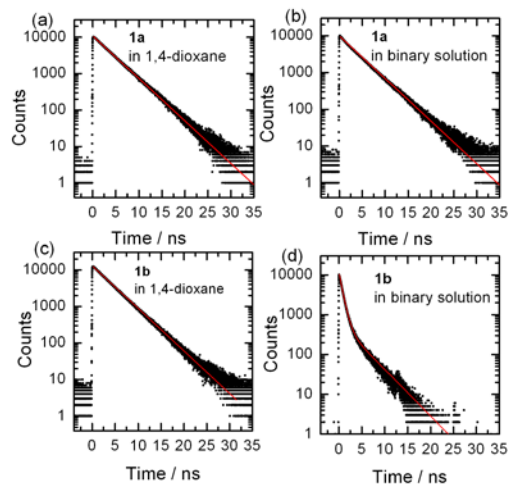


Figure 4. Fluorescence time profiles of the open- (**1a**) and closed-ring (**1b**) isomers in pure 1,4-dioxane solution, (a) and (b), and in a binary solvent (1,4-dioxane/methanol = 50/50), (c) and (d). The excitation and monitoring wavelength were 532 nm and 540 nm, respectively. Instrumental response function (IRF) was 32 ps. Solid lines are results calculated for the analysis (see text).

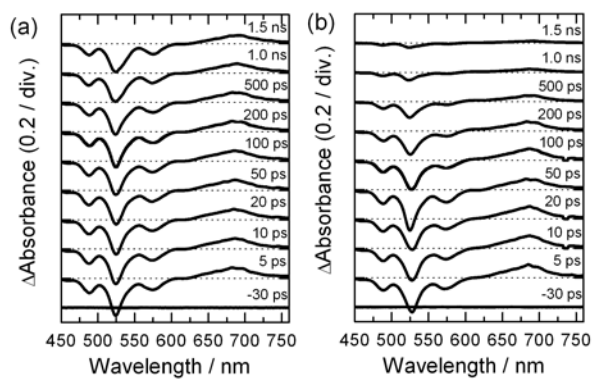


Figure 5. Time-resolved transient absorption spectra of the closed-ring isomer (**1b**), excited with a fs 530 nm laser pulse; (a) in pure 1,4-dioxane solution and (b) in a binary solvent (1,4-dioxane/methanol = 50/50).

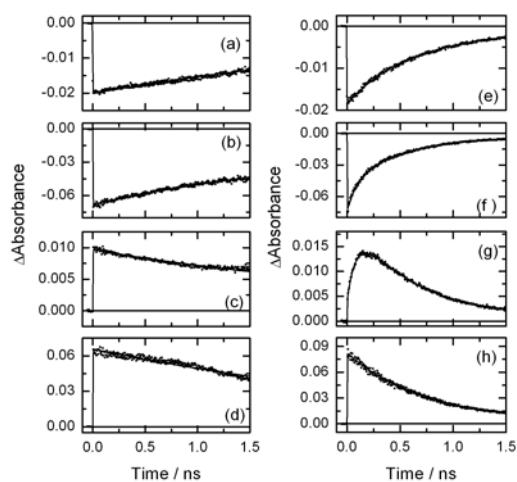


Figure 6. Time profiles of transient absorbance of the closed-ring isomer (**1b**), excited with a fs 530 nm laser pulse; (a)-(d) observed in pure 1,4-dioxane solution and (e)-(h) in a binary solvent (1,4-dioxane/methanol = 50/50). The detection wavelength is 470 nm for (a) and (e), 570 nm for (b) and (f), 620 nm for (c) and (g), and 680 nm for (d) and (h). Solid lines in each of the frames are calculated curves by taking into account the pulse durations and the time constants.

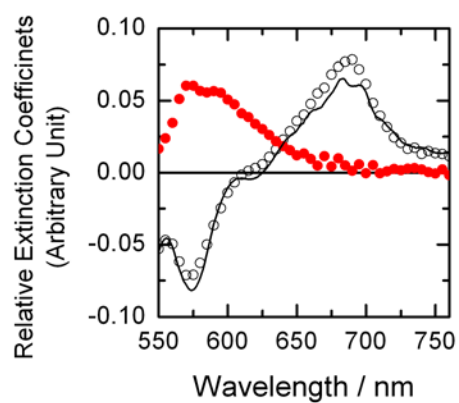


Figure 7. Wavelength dependence of the molar extinction coefficients for the precursor species *A* (open circles) and the successor species *B* (closed circles), obtained by analysis of the time profiles of transient absorption of the closed-ring isomer (**1b**) in a binary solvent (1,4-dioxane/methanol = 50/50) (see text). Solid line is the transient absorption spectrum of **1b** in pure 1,4-dioxane solution.